Japanese Journal of Applied Physics **50** (2011) 031001 **REGULAR PAPER**
DOI: 10.1143/JJAP.50.031001

Ternary AlGaN Alloys with High Al Content and Enhanced Compositional Homogeneity Grown by Plasma-Assisted Molecular Beam Epitaxy

Vincent Fellmann[1,2], Périne Jaffrennou[1], Diane Sam-Giao[1], Bruno Gayral[1], Katharina Lorenz[3], Eduardo Alves[3], and Bruno Daudin[1]

[1]*CEA-CNRS Group "NanoPhysique et SemiConducteurs", INAC/SP2M/NPSC, CEA-Grenoble, 17 rue des Martyrs, 38054 Grenoble, Cedex 9, France*
[2]*ACERDE, 452 Rue des Sources, F-38920 Crolles, France*
[3]*Instituto Technológico e Nuclear, Estrada Nacional 10, Sacavém 2686-953, Portugal*

Received June 7, 2010; accepted November 12, 2010; published online March 22, 2011

We have studied the influence of III/N flux ratio and growth temperature on structural and optical properties of high Al-content, around 50–60%, AlGaN alloy layers grown by plasma-assisted molecular beam epitaxy. In a first part, based on structural analysis by Rutherford Backscattering Spectroscopy, we establish that a III/N flux ratio slightly above 1 produces layers with low amount of structural defects. In a second part, we study the effect of growth temperature on structural and optical properties of layers grown with previously determined optimal III/N flux ratio. We find that optimal growth temperatures for $Al_{0.50}Ga_{0.50}N$ layers with compositional homogeneity related with narrow UV photoluminescence properties are in the low temperature range for growing GaN layers, i.e., 650–680 °C. We propose that lowering Ga adatom diffusion on the surface favors random incorporation of both Ga and Al adatoms on wurtzite crystallographic sites leading to the formation of an homogeneous alloy.

1. Introduction

The current interest in UV light emitting diodes (LED) is strongly driven by applications. This statement is particularly true for the UV-C range (4.3–6.2 eV/200–290 nm) due to the high bactericidal potential of photons in this wavelength range. However, the control of efficient UV LED growth still remains challenging due to several difficulties which have been recently reviewed.[1)] In the case of UV-C emission, growth control of $Al_xGa_{1-x}N/Al_yGa_{1-y}N$ heterostructures is required. Such heterostructures provide a certain degree of freedom since, for a given barrier composition, quantum well (QW) emission can be tuned either by its composition or by its thickness. However, thin QWs are generally preferred to minimize the effect of the internal electric field. Accordingly, LED emitting around 255 nm have already been reported with active layers composed of a few nm thick $Al_{0.6}Ga_{0.4}N$ multi-quantum wells (MQWs) between thicker AlGaN barriers with Al contents ranging from 0.75 to 0.65.[2–4)] As a matter of fact, emission in this region of the optical spectrum requires high Al content AlGaN layers for both QWs and barriers (in the 0.5–0.8 range). Therefore, mastering of AlGaN nitride ternary alloys is of tremendous importance for the properties of such UV light emitting devices. Related to this statement, a practical challenge to overcome in order to grow efficient UV LEDs is to control the crystallographic quality of the barriers and QWs.

Control of the structural properties of such nitride ternary alloys is not straightforward since dislocation density in nitride binary alloys, i.e., GaN and AlN, is correlated to grain size and, consequently, to adatom mobility.[5)] For instance, for a growth temperature of about 1050–1100 °C, metal organic vapor deposition (MOCVD) GaN layers exhibit a dislocation density typically ranging in the $10^8/cm^2$ whereas AlN grown at the same temperature presents a far higher dislocation density, about $10^{10}/cm^2$. The question then arises to determine what should be the optimal growth temperature for Al-rich AlGaN due to potential alloy inhomogeneities or defects coming from the difference between Ga and Al adatom mean free paths. In addition, whatever the growth temperature, the differences in mean free path and strain between Al- and Ga-rich regions are expected to favour phase separation.[6,7)] This does not only hold for MOCVD growth process but also for molecular beam epitaxy (MBE) since the typical growth temperatures in this technique, i.e., 750–850 °C, correspond to relatively high Ga mobility on the surface, but almost no Al diffusion.

In previous studies, the growth conditions generally used for $Al_xGa_{1-x}N$ with low Al-content grown by plasma-assisted (PA) MBE were slightly Ga-rich conditions combined with substrate temperature above 750 °C.[8)] It is well known that, in the case of binary alloy (GaN or AlN) as well as for AlGaN ternary layers with low Al-content, such conditions produce samples with atomically smooth surface whereas N-rich conditions and moderate growth temperatures lead to rough surfaces.[9)] For higher Al-contents ($0.4 < x < 0.6$), it has been shown by Jmerick *et al.* that layers with smooth surfaces were obtained for a growth temperature of 700–710 °C and metal-rich flux ratio.[10)] They also noticed that such growth condition lead to more homogeneous layers,[11)] as compared to inhomogeneous layers with three dimensional morphology elaborated by Sampath *et al.* in N-rich growth conditions.[12)]

One goal of this article is to address systematically the issue of growth conditions on alloy homogeneity in the case of $Al_xGa_{1-x}N$ layers with high Al-content around 50% elaborated by PA-MBE. As adatom mobility can be modified either by growth temperature or by tuning the III/N flux ratio, the role of both parameters has been investigated by means of structural and optical characterizations of several samples.

Indeed, we will show that in PA-MBE the requirements for growing Al-rich AlGaN with reduced composition fluctuations characteristic of an homogeneous alloy correspond to slightly Ga-rich conditions and substrate temperatures around 650 °C.

2. Experimental Methods

The AlGaN layers have been grown by PA-MBE on 1-μm-thick AlN on sapphire (0001) pseudo-substrates

Table I. Sample description for AlGaN layers with Al content around 50% and Al/Ga flux ratio of 1. III/N flux ratio, growth temperature as well as Ga and Al cell temperatures are indicated. Results from RBS channelling are also shown.

	N-rich	Stoichiometry	Metal-rich
III/N ratio	0.85	1	1.2
Growth temperature (°C)	692–697	703–707	680
Ga/Al cell temperature (°C)	850/1120	855/1125	860/1130
Al content by RBS (%)	49	50	54
χ_{min} Ga (%)	3	3	8

(commercial DOWA substrates). Active nitrogen was supplied by a radiofrequency plasma source with a plasma power of 350 W, which leads to a growth rate of 0.25 ML/s at stoichiometry, i.e., around 220 nm per hour.

Active N flux was kept constant from sample to sample. Metallic species were provided by Knudsen cells. Before growth, substrates were chemically cleaned by a standard method and outgassed at 700 °C. An AlN buffer layer grown at high temperature was first deposited under Al-rich conditions before further growth of 0.3–0.4 μm thick AlGaN layers. It has to be noted that GaN substrates were not chosen because of the larger lattice mismatch with Al-rich AlGaN and because they are detrimental to photoluminescence (PL) and absorption experiments. The growth morphology of the layers has been followed *in situ* by reflection high energy electron diffraction (RHEED). III/N flux ratios were determined by RHEED oscillation calibrations at moderate growth temperature for GaN (around 700 °C) and high temperature for AlN (around 750 °C).

In order to investigate the role of III/N flux ratio and growth temperature on the structural and optical properties of Al-rich AlGaN, we have grown and analyzed two series of AlGaN samples with different growth conditions. The growth conditions of the first series are described in Table I. These samples allowed us to investigate the influence of III/N flux ratio on structural properties of $Al_{0.50}Ga_{0.50}N$. The second series consists of nine $Al_{0.55}Ga_{0.45}N$ layers grown at various growth temperatures, ranging from 540 °C to 760 °C, using an optimized III/N flux ratio of 1.08. It was realized to compare the influence of growth temperature on structural and optical properties of AlGaN.

Structural properties of AlGaN layers were analyzed by Rutherford backscattering spectrometry/channelling (RBS/C). These measurements were performed using a 2 MeV α particle beam, a two-axis goniometer and two detectors mounted at backscattering angles of 140 and 180°. We used a channelling configuration with alignment along the ⟨0001⟩ axis in order to quantitatively measure the alloy crystal quality. Random spectra were taken by tilting the sample away from the aligned position by 5° and rotating it during the measurement. In particular, we have determined the minimum yield (χ_{min}) for Ga close to the sample surface for all samples. This value is related to the amount of interstitial crystallographic defects in the material and is defined as the ratio between the backscattering yields of the aligned and random spectra. Small minimum yield is thus correlated with low structural defect density. The random spectra have been fitted using the NDF code to determine compositions and layer thicknesses.[13)]

Additional structural analysis has been performed with a three-axis high resolution X-ray diffraction (HRXRD) setup using a Ge(220) four-bounce monochromator in front of a beam concentrator. Furthermore, Sollers slits or a Ge(220) two-bounce analyzer were used in front of the detector.

Surface roughness of the grown layers was analyzed by atomic force microscopy (AFM). AFM micrographs in tapping mode have also been realized. Root mean square measurements (RMS) have been performed with WSxM software on $5 \times 5\,\mu m^2$ images.[14)] A continuous decrease of the RMS values, down to 1.9 nm, is observed when decreasing the growth temperature from 760 to 600 °C. No RMS values could be extracted for the samples grown at temperature lower than 600 °C because of the presence of a high content of Ga droplets on the surface, due to the very low Ga desorption. For substrate temperature above 720 °C, we can attribute the strong surface roughness (RMS > 10 nm) to increased Ga desorption resulting into N-rich growth conditions. For substrate temperature below 680 °C, we can observe hillocks nucleated around dislocations. Such hillocks have already been observed in GaN[15)] and in InGaN[16)] and have been related to enhanced Ga diffusion under Ga-rich conditions.[17)] In the present case of AlGaN, it is suggested that the presence of hillocks is associated with Ga accumulation, in slightly Ga-rich conditions. Finally, for very low substrate temperature (below 650 °C) and concomitantly very low desorption rate, we observe the presence of metal droplets on the surface.

Optical properties of AlGaN were investigated by optical absorption and PL spectroscopies. Optical transmission experiments were performed at room temperature. A high pressure xenon lamp filtered by a double monochromator was shone on the sample. The filtered light was tuned from 230 to 380 nm with a 1 nm pitch. The light transmitted across the sample was detected by a photon counting photomultiplier. The transmission spectra were then normalized by the spectrum obtained with no sample in the light path.

UV emissions have been analyzed with a macro-PL setup. The excitation source was a continuous frequency-doubled argon laser at 244 nm (5.08 eV). The signal was dispersed in a 460 mm focal length monochromator equipped with a 600 grooves/mm grating and detected by a nitrogen-cooled charge-coupled device (CCD) camera. Samples were mounted in a He-flow cryostat offering the possibility to adjust the temperature from 4 K to room temperature (RT).

3. Results

3.1 Structural properties

3.1.1 Influence of III/N flux ratio

Reports dealing with the influence of III/N flux ratio on crystallographic structure and surface morphology of III–N ternary alloys are scarce in literature.[18)] Thus, in order to determine the optimum III/N flux ratio for Al-rich AlGaN layers grown by PA-MBE, we have analyzed the structural properties of the first series of samples (Table I) grown with three different III/N flux ratios: under N-rich conditions, i.e., with III/N < 1; under metal-rich conditions, i.e., with III/N > 1; and at stoichiometry. The metal flux of Ga (Al) was determined by measuring RHEED oscillations on GaN (AlN) layers homoepitaxially grown on GaN and AlN MOCVD templates, respectively. In addition, it is worth

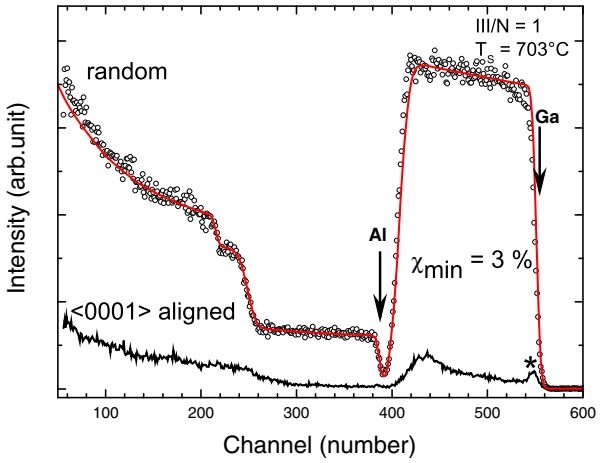

Fig. 1. (Color online) ⟨0001⟩ aligned and fitted random RBS/C spectra for sample grown at stoichiometry. Arrows indicate the position of Ga and Al signals from the surface for AlGaN layer; the star indicates surface peak.

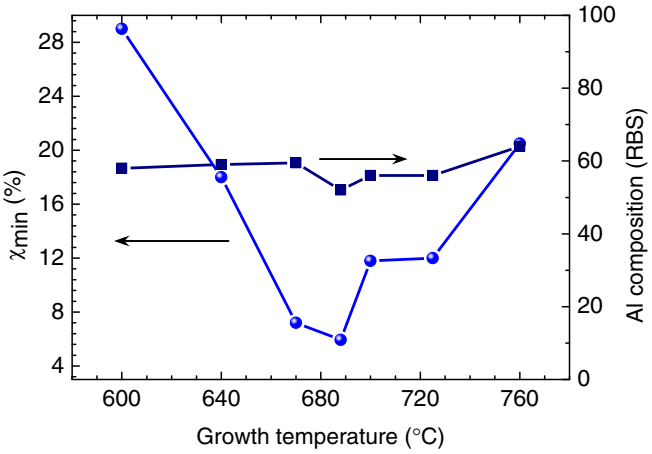

Fig. 2. (Color online) χ_{min} for Ga (left) and Al contents (right) as determined from RBS/C measurements. Growth temperatures of AlGaN layers vary from 600 to 760 °C under stoichiometric conditions.

mentioning that the effects of growth temperature on Ga desorption were neglected for the determination of III/N ratio from RHEED oscillations, as well as the differences between Al–N and Ga–N bonds on incorporation probabilities during the formation of AlGaN ternary alloys. We have thus focused our attention on metal/N ratios values in the 0.8–1.2 range for samples grown at a medium substrate temperature (around 700 °C) in order to limit Ga desorption. It has to be stressed out that the Al/Ga ratio was kept constant from sample to sample.

The RBS/C results for these AlGaN samples are presented in Table I. We measured a minimum yield (χ_{min}) of 3% for the samples grown under N-rich conditions and at stoichiometry, whereas the sample grown under Ga-rich conditions shows a poorer value, with a χ_{min} of 8%. Figure 1 shows RBS/C random and aligned spectra for the sample grown at stoichiometry. As expected, the backscattering yield in the aligned configuration is strongly reduced as compared to the random configuration, which indicates marked channelling effect. The χ_{min} of 3% in the energy window corresponding to Ga atoms close to the surface reveals the excellent crystal quality of the alloy film. As a further indication of structural quality, a surface peak is clearly seen in the aligned spectrum. It can be emphasized that the measured χ_{min} value of a few percents is comparable to what is already reported for the best AlGaN layers grown by MOCVD. Indeed, Schowalter *et al.* have measured χ_{min} of 2.2% for *a*-plane $Al_{0.50}Ga_{0.50}N$ whereas a χ_{min} of 2.7% has been reported for *c*-plane $Al_{0.42}Ga_{0.58}N$ thick films grown on GaN.[19,20] These values have to be compared with χ_{min} values of 1.5%, for *a*-plane AlN and 1.4% for *c*-plane GaN reported for layers grown by MOCVD.[19]

From our RBS/C minimum yield measurements, it can be partially concluded that $Al_{0.50}Ga_{0.50}N$ crystal layers with best structural quality are grown under a III/N flux ratio between 0.85 and 1.

3.1.2 Influence of growth temperature

As growth temperature is expected to have a significant influence on crystal quality, we have grown a series of samples with substrate temperatures ranging from 540 to 760 °C. Based on the above results on III/N flux ratio influence, we have chosen to use a III/N flux ratio close to stoichiometry. It has to be noted that sample grown at highest temperature show characteristic features of N-rich growth conditions, notably a large surface roughness. We have analyzed these samples in RBS/C and we have determined their χ_{min} values and their Al content (Fig. 2). It is interesting to note that the measured Al molar fraction for growth temperature between 680 and 760 °C, around 50–60%, is slightly increasing with growth temperature, which is due to enhanced Ga desorption at high temperature. Concerning the χ_{min} values, we can clearly observe a decrease when decreasing growth temperature from 760 to 650–680 °C while it is increasing again for substrate temperatures below 650 °C. In particular, for substrate temperatures around 660–680 °C, we report a χ_{min} value of 5%, which is a clear indication of a good crystalline quality. For substrate temperatures above 750 °C and below 620 °C, χ_{min} values are larger than 20%, indicating a degradation of the crystalline structure. More specifically, we measured χ_{min} values up to 75% at 540 °C, which is related to a very bad crystalline quality that may be due to the limited diffusion of both metallic species under these low growth temperature conditions.

Based on the above experimental data, it can be concluded that the best crystalline quality for $Al_{0.50}Ga_{0.50}N$ layers is obtained for III/N flux ratio around 1 and substrate temperatures around 650–680 °C. Interestingly, this temperature lies in the lower limit of optimal growth temperature range of GaN by MBE (650–750 °C), the upper value being limited by the decomposition rate of the deposited material.[21,22] It is remarkable that although the optimal growth temperature range for AlN is expected to be higher than for GaN due to the higher decomposition temperature of AlN, the optimum growth temperature for $Al_{0.50}Ga_{0.50}N$ is smaller than the one for each binary alloys.

Additionally, structural quality has also been investigated by HRXRD full width at half maximum (FWHM) measurements on the symmetric 0002 reflection. It has to be noticed that AlGaN ω–2θ peaks show asymmetry which can be related to partial strain relaxation. Ternary AlGaN layers with ⟨0001⟩ orientation have by nature columnar grain structure

Table II. XRD FWHM measured on symmetric 0002 reflections for $T_s = 760$ and 670 °C (III/N = 1.08). Values for AlN correspond to substrate or buffer layer. Also shown data from other groups for AlGaN layers grown with various methods with Al content around 50%.

Al-content (substrates)	$\Delta(2\theta–\omega)$ AlGaN (arcsec)	$\Delta(2\theta–\omega)$ AlN (arcsec)	$\Delta\omega$ AlGaN (arcsec)	$\Delta\omega$ AlN (arcsec)	Reference
$Al_{0.60}Ga_{0.40}N$ $T_S = 760$ °C PA-MBE (AlN/Al_2O_3)	461	78	593	240	This work
$Al_{0.64}Ga_{0.46}N$ $T_S = 670$ °C PA-MBE (AlN/Al_2O_3)	595	88	630	150	This work
AlN/Al_2O_3 MOCVD				50–100	This work (templates)
$Al_{0.46}Ga_{0.54}N$ PA-MBE (GaN/Al_2O_3)	240	30	475	290	24
$Al_{0.46}Ga_{0.54}N$ PA-MBE (AlN/Al_2O_3)	230	55	890	75	24
$Al_{0.60}Ga_{0.40}N$ PA-MBE (AlN/Al_2O_3)			400		25
$Al_{0.67}Ga_{0.33}N$ PA-MBE (AlN/Al_2O_3)	590	55	320	75	24
$Al_{0.54}Ga_{0.46}N$ MOCVD (AlN/Al_2O_3)			597		26
$Al_{0.58}Ga_{0.42}N$ NH_3-MBE ($AlGaN/Al_2O_3$)			1200		27
$Al_{0.5}Ga_{0.5}N$ MOCVD (bulk AlN)			200	36	28
$Al_{0.6}Ga_{0.4}N$ MOCVD (AlN/Al_2O_3)			300	40	29
$Al_{0.6}Ga_{0.4}N$ MOCVD (AlN/Al_2O_3)			250	80	29

which exhibits tilted and twisted misorientations. Relatively large values of FWHM for symmetric ω–2θ scans are related with intrinsic alloy disorder, i.e., the stochastic occupation of a sublattice site by an atom of Ga or Al. Symmetric ω-scans FWHM are related with columnar tilt, correlated with the density of screw and mixed dislocations.[23)]

Table II summarizes FWHM of ω–2θ and ω scans on symmetric 0002 reflection for two samples: one grown in N-rich growth conditions due to high growth temperature at 760 °C, the other one at optimized growth conditions (T_S = 670 °C), as well as values from literature.[24–29)] It has to be noticed that crystalline quality as measured by HRXRD is strongly dependent on the quality of the substrate, the strain state and the growth method used.

For the sample grown at 670 °C in slightly Ga-rich growth conditions, we report value of 630 arcsec for rocking scan on the 0002 reflection. This value is remarkably close to the ones reported in Table II for AlGaN layers with similar Al content grown by PA-MBE[24)] and MOCVD.[26)]

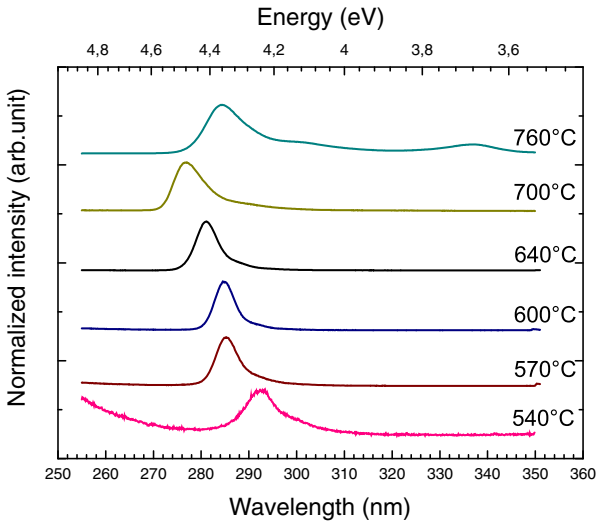

Fig. 3. (Color online) Normalized PL spectra at $T = 7$ K for AlGaN layers grown at temperatures from 540 to 760 °C.

In summary, by contrast to what could be expected by a naive extrapolation of optimal growth conditions for GaN and AlN, we have determined from RBS/C measurements that optimal growth conditions for $Al_{0.50}Ga_{0.50}N$ in terms of alloy homogeneity are obtained for near stoichiometry conditions and a substrate temperature around 660 °C.

3.2 Optical properties

Absorption and emission properties of the $Al_{0.50}Ga_{0.50}N$ samples grown at different growth temperatures and under a III/N flux ratio of 1.08 have been studied by means of optical absorption and PL spectroscopies. As a first step, we have recorded RT optical absorption spectra of these samples (not shown here). For all samples, we have observed a clear absorption edge at 4.6–4.75 eV (260–270 nm) which can be correlated to the expected band gap of AlGaN containing 50% of Al and consistent with the RBS measurements reported above.[30)] The absorption spectra have also been compared to the PL spectra in order to unambiguously identify the PL emission as near band edge (NBE) emissions.

Figure 3 shows the PL spectra recorded at 7 K. For growth temperatures below 700 °C, the PL spectra are dominated by NBE emission around 4.4 eV (280 nm). Above 700 °C, we can observe the apparition of a shouldering at lower energy (~4.1 eV) and an additional band around 3.7 eV. This shouldering can be tentatively assigned to NBE emission of other AlGaN phases and the additional band to defects or impurity bands.[31,32)] The clear asymmetric shape toward low energy of samples grown above 700 °C could be related to localized exciton states.

In Fig. 4, we observe that the FWHM of the NBE signals changes with growth temperature. Interestingly, the FWHM clearly narrows with decreasing substrate temperatures until 600 °C and then widens while further lowering temperature. For a growth temperature of 600 °C, we report a narrowest FWHM value of 64 meV. In addition, we can mention that we observed a decrease of PL intensity emissions for samples grown below 650 °C. Then, consistent with the fact that a narrow NBE FWHM is a sign of a high degree of

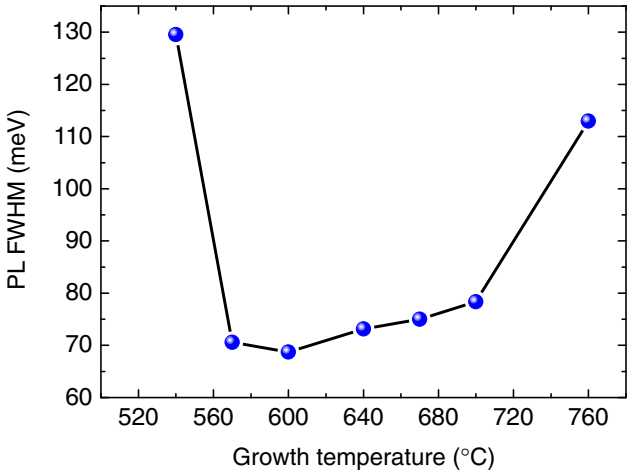

Fig. 4. (Color online) Measured PL FWHM at $T = 7$ K of NBE emissions from Fig. 3. FWHM have been estimated from lineshape analysis with multi-gaussian fitting and minimization of the χ^2 value.

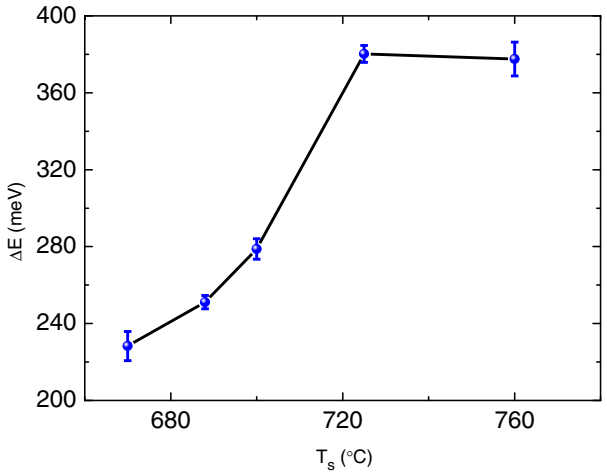

Fig. 5. (Color online) Estimated Stokes-like shift ΔE from Fig. 3 and absorption spectra (not shown).

crystal homogeneity and that high intensity PL signals are observed in good crystalline quality alloys, it appears that the best emission properties are obtained for the AlGaN layers grown around 650 °C, which is in good agreement with the structural results.

As for the PL spectra of the samples grown at temperatures lower than 700 °C, we can notice that the energy positions of the NBE signals slightly decrease with decreasing substrate temperature. This is assigned to a decrease of AlGaN bandgap with lower substrate temperature, which is confirmed by the variation of the optical absorption edge which is a better measurement of the band gap value of the ternary alloy. This is consistent with a slight increase of the Ga content in the AlGaN alloys at lower substrate temperature, as confirmed by RBS compositional analysis.

The combined analysis of absorption and PL results can bring more insight on the homogeneity of the AlGaN alloy. Figure 5 shows the variation of the Stokes shift (energy difference between the absorption edge and the PL peak) as a function of growth temperature. In order to take into account the increase of AlGaN bandgap with temperature between 7 and 300 K, all absorption measurements have been corrected by an energy shift of 65 meV.[33] As a matter of fact, Stokes shift in ternary alloys is a well known measure of the energy difference between localized states with low Al content and extended states which reflect the average Al content.[34] As localization in III–N materials can occur at the nanometer scale, often not directly accessible by structural characterization, the optical measure of the Stokes shift can be seen as a probe of ternary alloy potential fluctuations. In the present case, we observe that when increasing the growth temperature from 670 to 725 °C, the Stokes shift increases considerably, thus showing that the short-scale composition fluctuations are accentuated at higher temperature, in line with the RBS measurements. Sample grown at 760 °C in N-rich conditions exhibits stronger Stokes shift, consistent with the presence of nanometer scale compositional inhomogeneities.[35]

4. Discussion

From structural and optical analysis of AlGaN samples reported above, it can be concluded that optimum growth conditions for $Al_{0.50}Ga_{0.50}N$ layers correspond to a III/N flux ratio around 1 and a substrate temperature around 650 °C.

Indeed, III/N flux ratio has already been identified as a key parameter for growing high quality GaN and AlN layers by PA-MBE. In both cases, assuming that growth temperature is high enough to promote adatom diffusion, good surface and crystallographic qualities are obtained with an excess of Ga/Al on the growth front (Ga/N, Al/N > 1). Theoretical calculations as well as experiments show that, in this case, metallic Ga/Al adlayers are stabilized on the surface.[36,37] This metallic excess acts as a surfactant on the surface and improves the Ga/Al adatom diffusion. Good AlN quality is thus related to Al adatom diffusion which can be improved by using Al-rich growth conditions and high growth temperature (i.e., 750–850 °C). A similar mechanism has been observed in the case of GaN, with the formation of a metallic Ga bilayer on the growth front, which acts as a channel for N adatom diffusion.[36] Nevertheless, due to the high desorption rate of Ga at temperature above 750 °C, growth has to be performed at lower temperatures than for AlN, i.e., below 750 °C.

In the case of AlGaN growth, the hypothetical existence of a stable adlayer has not been established. In the absence of metallic adlayer, it is expected that the growth window between a regime with Ga accumulation on the surface and N-rich growth condition is very narrow, making growth difficult in a steady state regime. As a matter of fact, this is consistent with the experimental observation that a change of only a few degrees of the Ga cell temperature is sufficient to switch from one regime to another. Interestingly, for Al-rich AlGaN material, it has been found by Bhattacharyya *et al.* that metal-rich conditions are associated with compositional inhomogeneities leading to an increase of the PL FWHM.[6] In addition, it has to be emphasized that the growth temperature chosen by these authors was in the range of 750–800 °C[6,38] which, based on our results, is expected to have a negative impact on PL FWHM.

In summary, we have established that AlGaN layers with good compositional homogeneities are obtained by using III/N flux ratio close to stoichiometry and low growth temperatures in order to decrease adatom diffusion while promoting random incorporation of Al and Ga. Along these lines, theoretical studies by Albrecht *et al.* have shown that, by contrast, ordered structures are kinetically driven for $Al_{50}Ga_{50}N$ alloys: high substrate temperature enhances adatom diffusion to step edges or vicinal facets. These authors have also shown that such chemical ordering leads to an increase of the cathodoluminescence FWHM as well as to a redshift of the luminescence.[39] Furthermore, an additional carrier localization mechanism without ordering (designated as NCIs for nanoscale compositional inhomogeneities) has been proposed.[12,40] Such a mechanism could possibly occur in AlGaN films grown at high temperature with III/N flux ratio below unity.[12]

Then, it can be postulated that low growth temperature for AlGaN is associated to the formation of an "ideally" random alloy, while limiting possible Al or Ga segregation. However, on one hand growth temperature cannot be arbitrarily decreased below a value which would result in insufficient adatom diffusion. Indeed an increase of the χ_{min} values is observed for temperatures below 620 °C, possibly due to interstitial Al/Ga, dislocations or point defect clusters. On the other hand, growth temperature under 700 °C may lead to Ga droplet formation on the AlGaN surface due to unsufficient Ga evaporation during growth,[41] further emphasizing the sharpness of the growth window between metal- and N-rich growth conditions.

Concerning optical results, our best sample showing a FWHM of 64 meV for Al-content of 58% is expected to present a high degree of compositional *disorder*, i.e., a high degree of alloy *homogeneity*, as the prediction for a completely homogeneous alloy with similar Al-content is about 40 meV.[42–44] It is interesting to notice that Nam *et al.* report FWHM of 50 and 55 meV for AlGaN alloy grown by MOCVD with Al content of 50 and 70%, respectively.[45] Our AlGaN layers grown under optimized conditions by PA-MBE have FWHM comparable to these state of the art AlGaN layers and are approaching theoretical PL properties of random AlGaN alloys.[44,46] Interestingly, it should be noted that in the somewhat different case of metal organic vapor phase epitaxy, "low" growth temperature has been found to decrease adatom mobilities and to increase alloy homogeneity.[47] Furthermore, linewidth emission from GaN/AlGaN QW was found to be narrowed, which was assigned to reduced Al-content fluctuations, as a clue that such a fluctuation reduction is essential to optimized AlGaN-based heterostructures growth, consistent with results introduced in the present article.

5. Conclusions

In conclusion, we have shown that surface morphology and composition homogeneity as well as optical properties of $Al_{0.50}Ga_{0.50}N$ grown by PA-MBE are highly sensitive to growth conditions, and more specifically to III/N flux ratio and growth temperature. Based on structural and optical characterizations, we have pointed out that homogeneous $Al_{0.50}Ga_{0.50}N$ alloys can be grown with III/N flux ratio close to unity and growth temperatures in the range 650–680 °C. Such growth temperature is in the low temperature range of typical growth conditions for GaN layers and far below typical AlN growth temperature. We postulate that, for growing homogeneous AlGaN alloys, limited Ga adatom diffusion induced by the low growth temperature favors random incorporation on the growth front of both metallic species, whereas high Ga or Al diffusion is required to optimize binary alloys growth. For such $Al_{0.50}Ga_{0.50}N$ grown under optimized growth conditions, we report a good crystalline quality with low surface roughness and narrow UV PL emission lines. These results concerning Al-rich alloys grown by PA-MBE open new insights for the optimization of $Al_xGa_{1-x}N/Al_yGa_{1-y}N$ heterostructures and for deep UV LED realization.

Acknowledgments

Authors greatly acknowledge Y. Curé for technical assistance and Dr. E. Bellet-Amalric for support in HRXRD experiments. This work has been supported by the ANR PNANO project DUVED, the FCT Portugal (PTDC/FIS/65233/2006, ciência 2007), and the bilateral collaboration program PESSOA (EGIDE/GRICES).

1) A. Khan, K. Balakrishnan, and T. Katona: Nat. Photonics **2** (2008) 77.
2) H. Hirayama, S. Fujikawa, N. Noguchi, J. Norimatsu, T. Takano, K. Tsubaki, and N. Kamata: Phys. Status Solidi A **206** (2009) 1176.
3) V. Adivarahan, W. H. Sun, A. Chitnis, M. Shatalov, S. Wu, H. P. Maruska, and M. Asif Khan: Appl. Phys. Lett. **85** (2004) 2175.
4) W. Sun, M. Shatalov, J. Deng, X. Hu, J. Yang, A. Lunes, Y. Bilenko, M. Sur, and R. Gaska: Appl. Phys. Lett. **96** (2010) 061102.
5) T. Böttcher, S. Einfeldt, S. Figge, R. Chierchia, H. Heinke, and D. Hommel: Appl. Phys. Lett. **78** (2001) 1976.
6) A. Bhattacharyya, T. D. Moustakas, L. Zhou, D. J. Smith, and W. Hug: Appl. Phys. Lett. **94** (2009) 181907.
7) A. Wise, R. Nandivada, B. Strawbridge, R. Carpenter, N. Newman, and S. Mahajan: Appl. Phys. Lett. **92** (2008) 261914.
8) K. Nozawa, N. Maeda, Y. Hirayama, and N. Kobayashi: J. Cryst. Growth **189–190** (1998) 114.
9) F. Widmann, B. Daudin, G. Feuillet, N. Pelekanos, and J. L. Rouvière: Appl. Phys. Lett. **73** (1998) 2642.
10) V. N. Jmerik, A. M. Mizerov, T. S. Shubina, A. V. Sakharov, A. A. Sitnikova, P. S. Kop'ev, S. V. Ivanov, E. V. Lutsenko, A. V. Danilchyk, N. V. Rzheutskii, and G. P. Yablonskii: Semiconductors **42** (2008) 1420.
11) V. N. Jmerik, T. V. Shubina, A. M. Mizerov, K. G. Belyaev, A. V. Sakharov, M. V. Zamoryanskaya, A. A. Sitnikova, V. Yu. Davydov, P. S. Kop'ev, E. V. Lutsenko, N. V. Rzheutskii, A. V. Danilchik, G. P. Yablonskii, and S. V. Ivanov: J. Cryst. Growth **311** (2009) 2080.
12) A. V. Sampath, G. A. Garrett, C. J. Collins, W. L. Sarney, E. D. Readinger, P. G. Newman, H. Shen, and M. Wraback: J. Electron. Mater. **35** (2006) 641.
13) N. P. Barradas, C. Jeynes, and R. P. Webb: Appl. Phys. Lett. **71** (1997) 291.
14) I. Horcas, R. Fernandez, J. M. Gomez-Rodriguez, J. Colchero, J. Gomez-Herrero, and A. M. Baro: Rev. Sci. Instrum. **78** (2007) 013705.
15) T. Andreev, N. Q. Liem, Y. Hori, M. Tanaka, O. Oda, B. Daudin, and D. Le Si Dang: Opt. Mater. **28** (2006) 775.
16) S. Keller, U. K. Mishra, S. P. Denbaars, and W. Seifert: Jpn. J. Appl. Phys. **37** (1998) L431.
17) B. Liu, R. Zhang, Z. L. Xie, Q. J. Liu, Z. Zhang, Y. Li, X. Q. Xiu, J. Yao, Q. Mei, H. Zhao, P. Han, H. Lu, P. Chen, S. L. Gu, Y. Shi, Y. D. Zheng, W. Y. Cheung, N. Ke, and J. B. Xu: J. Cryst. Growth **310** (2008) 4499.
18) L. He, M. A. Reshchikov, F. Yun, D. Huang, T. King, and H. Morkoç: Appl. Phys. Lett. **81** (2002) 2178.
19) L. J. Schowalter, J. C. Rojo, G. A. Slack, Y. Shusterman, R. Wang, I. Bhat, and G. Arunmozhi: J. Cryst. Growth **211** (2000) 78.
20) J. C. Zhang, M. F. Wu, J. F. Wang, J. P. Liu, Y. T. Wang, J. Chen, R. Q. Jin, and H. Yang: J. Cryst. Growth **270** (2004) 289.
21) S. Fernández-Garrido, G. Koblmüller, E. Calleja, and J. Speck: J. Appl. Phys. **104** (2008) 033541.

22) S. Fernández-Garrido, A. Redondo-Cubero, R. Gago, F. Bertram, J. Christen, E. Luna, A. Trampero, J. Pereiro, E. Muñoz, and E. Calleja: J. Appl. Phys. **104** (2008) 083510.
23) M. A. Moram and M. E. Vickers: Rep. Prog. Phys. **72** (2009) 036502.
24) E. Monroy, B. Daudin, E. Bellet-Amalric, N. Gogneau, D. Jalabert, F. Enjalbert, J. Brault, J. Barjon, and L. S. Dang: J. Appl. Phys. **93** (2003) 1550.
25) E. Monroy, F. Guillot, S. Leconte, E. Bellet-Amalric, E. Baumann, F. Giorgetta, D. Hofstetter, L. Nevou, M. Tchernycheva, L. Doyennette, F. H. Julien, T. Remmele, and M. Albrecht: Superlattices Microstruct. **40** (2006) 418.
26) X. Y. Wang, X. L. Wang, G. X. Hu, B. Z. Wang, Z. Y. Ma, H. L. Xiao, C. M. Wang, J. X. Ran, and J. P. Li: Microelectron. J. **38** (2007) 838.
27) X. Y. Wang, X. L. Wang, B. Z. Wang, H. L. Xiao, H. X. Liu, J. X. Wang, Y. P. Zeng, and J. M. Li: Phys. Status Solidi A **204** (2007) 3405.
28) Z. Ren, Q. Sun, S.-Y. Kwon, J. Han, K. Davitt, Y. K. Song, A. V. Nurmikko, H.-K. Cho, W. Liu, J. A. Smart, and L. J. Schowalter: Appl. Phys. Lett. **91** (2007) 051116.
29) Y. Sakai, Y. Zhu, S. Sumiya, M. Miyoshi, M. Tanaka, and T. Egawa: Jpn. J. Appl. Phys. **49** (2010) 022102.
30) E. Bellotti, F. Bertazzi, and M. Goano: J. Appl. Phys. **101** (2007) 123706.
31) N. Nepal, M. L. Nakarmi, J. Y. Lin, and H. X. Jiang: Appl. Phys. Lett. **89** (2006) 092107.
32) K. B. Nam, M. L. Nakarmi, J. Y. Lin, and H. X. Jiang: Appl. Phys. Lett. **86** (2005) 222108.
33) D. Brunner, H. Angerer, E. Bustarret, F. Freudenberg, R. Höpler, R. Dimitrov, O. Ambacher, and M. Stutzmann: J. Appl. Phys. **82** (1997) 5090.
34) H. Morkoç: *Handbook of Nitride Semiconductors and Devices* (Wiley-VCH, Weinheim, 2008) Vol. 2.
35) A. V. Sampath, G. A. Garret, E. D. Readinger, R. W. Enck, H. Shen, M. Wraback, J. R. Grandusky, and L. J. Schowalter: Solid-State Electron. **54** (2010) 1130.
36) J. Neugebauer, T. K. Zywietz, M. Scheffler, J. E. Northrup, H. Chen, and R. M. Feenstra: Phys. Rev. Lett. **90** (2003) 056101.
37) C. D. Lee, Y. Dong, R. M. Feenstra, J. E. Northrup, and J. Neugebauer: Phys. Rev. B **68** (2003) 205317.
38) Y. Wang, A. Özcan, K. F. Ludwig, Jr., A. Nhattacharyya, T. D. Moustakas, L. Zhou, and D. J. Smith: Appl. Phys. Lett. **88** (2006) 181915.
39) M. Albrecht, L. Lymperakis, J. Neugebauer, J. E. Northrup, L. Kirste, M. Leroux, I. Grzegory, S. Porowski, and H. P. Strunk: Phys. Rev. B **71** (2005) 035314.
40) C. J. Collins, A. V. Sampath, G. A. Garrett, W. L. Sarney, H. Shen, M. Wraback, A. Yu. Nikiforov, G. S. Cargill III, and V. Dierolf: Appl. Phys. Lett. **86** (2005) 031916.
41) S. Takigawa, K. Furuta, S. Shimizu, X.-Q. Shen, T. Kitamura, and H. Okumura: Jpn. J. Appl. Phys. **43** (2004) 952.
42) E. Kuokstis, W. H. Sun, M. Shatalov, J. W. Yang, and M. Asif Khan: Appl. Phys. Lett. **88** (2006) 261905.
43) N. Nepal, J. Li, M. L. Nakarmi, J. Y. Lin, and H. X. Jiang: Appl. Phys. Lett. **88** (2006) 062103.
44) G. Coli, K. K. Bajaj, J. Li, J. Y. Lin, and H. X. Jiang: Appl. Phys. Lett. **80** (2002) 2907.
45) K. B. Nam, J. Li, M. L. Nakarmi, J. Y. Lin, and H. X. Jiang: Appl. Phys. Lett. **84** (2004) 5264.
46) G. Coli, K. K. Bajaj, J. Li, J. Y. Lin, and H. X. Jiang: Appl. Phys. Lett. **78** (2001) 1829.
47) E. Feltin, D. Simeonov, J.-F. Carlin, R. Butté, and N. Grandjean: Appl. Phys. Lett. **90** (2007) 021905.